

The Zenith Angle Distribution of Fully Contained Events in SuperKamiokande and the Impact of Quasi Elastic Scattering on their Direction

E. Konishi¹, Y. Minorikawa², V.I. Galkin³,
M. Ishiwata⁴ and A. Misaki^{5,6}

December 2, 2018

¹ Department of Electronics and Information System Engineering, Hirosaki University, 036-8561, Hirosaki, Japan

² Department of Science, School of Science and Engineering, Kinki University, Higashi-Osaka, 577-8502, Japan

³ Department of Physics, Moscow State University, 119992, Moscow, Russia

⁴ Department of Physics, Saitama University, 338-8570, Saitama, Japan

⁵ Advanced Research Institute for Science and Engineering, Waseda University, 169-0092, Tokyo, Japan

⁶ Innovative Research Organization for the New Century, Saitama University, 338-8570, Saitama, Japan

Abstract

Quasi Elastic Scattering (QEL) is the dominant mechanism for producing both *Fully Contained Events* and *Partially Contained Events* in the SuperKamiokande (SK) detector for atmospheric neutrinos in the range ~ 0.1 GeV to ~ 10 GeV. In the analysis of SK events, it is assumed that the zenith angle of the incident neutrino is the same as that of the detected charged lepton.

In the present paper, we derive the distribution function for the scattering angle of charged leptons, the average scattering angles and their standard deviation due to QEL. Thus, it is shown that the SK

assumption for the scattering angle of the charged lepton in QEL is not valid. Further, for the rigorous analysis of the experimental data, the correspondence between the zenith angle of the charged leptons and that of the incident neutrinos should be examined by taking account of the influence of the azimuthal angle of the charged particle on its zenith angle. We conclude that it is not possible to reliably assign the zenith angle of the incident neutrino to that of the charged lepton, and so the zenith angle distribution of charged leptons under the SK assumption does not reflect that of the real incident neutrinos.

This result has clear implication for attempts to detect neutrino oscillations from the analyses of *Fully Contained Events* and *Partially Contained Events* in SuperKamiokande.

1 Introduction

The report of oscillations between muon and tau neutrinos for atmospheric neutrinos detected with SuperKamiokande (SK, hereafter) is claimed to be robustly established for the following reasons:

(1) The discrimination between electrons and muons in the SK energy range, say, ~ 0.1 GeV to ~ 1 GeV, has been proved to be almost perfect, as demonstrated by calibration using accelerator beams [1].

(2) The analysis, for both *Fully Contained Events* and *Partially Contained Events*, of the zenith angle distribution of electron-like (single ring) events and muon-like (single ring) events, based on the well established discrimination procedure mentioned in (1), reveals a significant deficit of muon-like events but the expected level of electron-like events. It is concluded that muon neutrinos oscillate into tau neutrinos which cannot be detected due to the small geometry of SK [2]. The analysis of SK data presently yields $\sin^2 2\theta > 0.89$ and $1.8 \times 10^{-3} \text{eV}^2 < \Delta m^2 < 4.5 \times 10^{-3} \text{eV}^2$ at 90% confidence level.¹

(3) The analysis of *Upward Through Going Events* and *Stopping Events*, in which the neutrino interactions occur outside the SK detector, leads to similar results to (2). The charged leptons which are produced in these categories are regarded as being exclusively muons, because electrons have negligible probabilities to produce such events as they lose energy very rapidly in the surrounding rock.

Thus for these events the discrimination procedure described in (1) is not required, and, therefore, the analysis here is independent of the analysis in (2).

¹The numerical values of the combination of $\sin^2 2\theta$ and δm^2 change from time to time. Here, we cite those from the most recent work [3].

For these events, however, the SK group obtains the same parameters for neutrino oscillations as in (2).²

The most robust evidence for neutrino oscillations is regarded as being that from the analysis of *Fully Contained Events*, because all details of the events are measured inside the detector and its analysis is free of the ambiguities that arise in the other analyses. *Partially Contained Events* have uncertainties due to their unknown ending points, and *Stopping Muon Events* and *Upward Through-Going Muon Events* both have uncertainties due to the unknown starting points, preventing a complete analysis of the events concerned.

In the SK experiment, the direction of the incident neutrino is assumed to be the same as that of the emitted charged lepton, i.e., the (anti-)muon or (anti-)electron, in the analysis of both *Fully Contained Events* and *Partially Contained Events* [3, 4]. However, as we will show, this assumption does not hold in the most important energy region, ~ 0.1 GeV to ~ 10 GeV, for both *Fully Contained Events* and *Partially Contained Events*, where Quasi Elastic Scattering (QEL) of the neutrino interaction is most dominant [5]. In the present paper, we examine the implication of this assumption in a quantitative way.

2 Cross Sections of Quasi Elastic Scattering in the Neutrino Reaction and the Scattering Angle of Charged Leptons.

We examine the following reactions due to the charged current interaction (c.c.).

$$\begin{aligned}\nu_e + n &\longrightarrow p + e^- \\ \nu_\mu + n &\longrightarrow p + \mu^- \\ \bar{\nu}_e + p &\longrightarrow n + e^+ \\ \bar{\nu}_\mu + p &\longrightarrow n + \mu^+\end{aligned}\tag{1}$$

The differential cross section for QEL is given as follows [6].

$$\frac{d\sigma}{dQ^2} = \frac{G_F^2 \cos^2 \theta_C}{8\pi E_\nu^2} \left\{ A(Q^2) \pm B(Q^2) \left[\frac{s-u}{M^2} \right] + C(Q^2) \left[\frac{s-u}{M^2} \right]^2 \right\}, \tag{2}$$

²It seems strange for different quality experimental data to give similarly precise results, because *Fully Contained Events* are of higher experimental quality compared with those of both *Upward Through Going Muon* and *Stopping Muon Events*. See also footnote 1.

where

$$\begin{aligned}
A(Q^2) &= \frac{Q^2}{4} \left[f_1^2 \left(\frac{Q^2}{M^2} - 4 \right) + f_1 f_2 \frac{4Q^2}{M^2} + f_2^2 \left(\frac{Q^2}{M^2} - \frac{Q^4}{4M^4} \right) + g_1^2 \left(4 + \frac{Q^2}{M^2} \right) \right], \\
B(Q^2) &= (f_1 + f_2) g_1 Q^2, \\
C(Q^2) &= \frac{M^2}{4} \left(f_1^2 + f_2^2 \frac{Q^2}{4M^2} + g_1^2 \right).
\end{aligned}$$

The signs $+$ and $-$ refer to $\nu_{\mu(e)}$ and $\bar{\nu}_{\mu(e)}$ for charged current (c.c.) interactions, respectively. The Q^2 denotes the four momentum transfer between the incident neutrino and the charged lepton. Details of other symbols are given in [6].

The relation among Q^2 , E_ν , the energy of the incident neutrino, E_ℓ , the energy of the emitted charged lepton (muon or electron or their anti-particles) and θ_s , the scattering angle of the charged lepton, is given as

$$Q^2 = 2E_\nu E_\ell (1 - \cos\theta_s). \quad (3)$$

Also, the energy of the charged lepton is given by

$$E_\ell = E_\nu - \frac{Q^2}{2M}. \quad (4)$$

In Figs. 1 to 4, we give the differential cross sections for different charged leptons and for different incident neutrino energies. It is clear from these figures that the cross sections of the neutrinos are larger than those of anti-neutrinos in the lower energy region, say, ~ 0.1 GeV to ~ 10 GeV and that their difference are negligible in higher energy region, say, beyond ~ 10 GeV. The differences between (anti-)muon and (anti-)electron are negligible except in the lower energy region, below ~ 0.1 GeV.

In Fig. 5, we give the total cross sections for muon neutrinos and anti-muon neutrinos. It can be seen that the differences between them are rather large in the lower energy region, say, ~ 0.1 GeV to ~ 10 GeV, but that the cross sections have similar values above ~ 10 GeV. The corresponding total cross sections for electron and positron are almost the same as those of the muon neutrinos and anti-muon neutrinos, respectively.

Now, let us examine the magnitude of the scattering angle of the charged lepton in a quantitative way, as this plays a decisive role in determining the accuracy of the direction of the incident neutrino, which is directly related to the reliability of the zenith angle distribution of both *Fully Contained Events* and *Partially Contained Events* in SK.

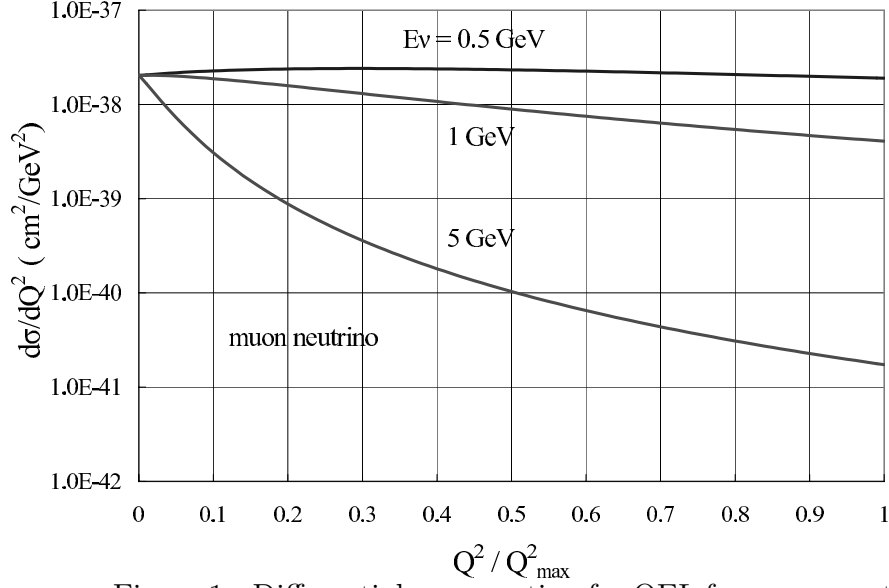


Figure 1: Differential cross section for QEL for muon neutrinos with different incident energies, 0.5 GeV, 1 GeV and 5 GeV.

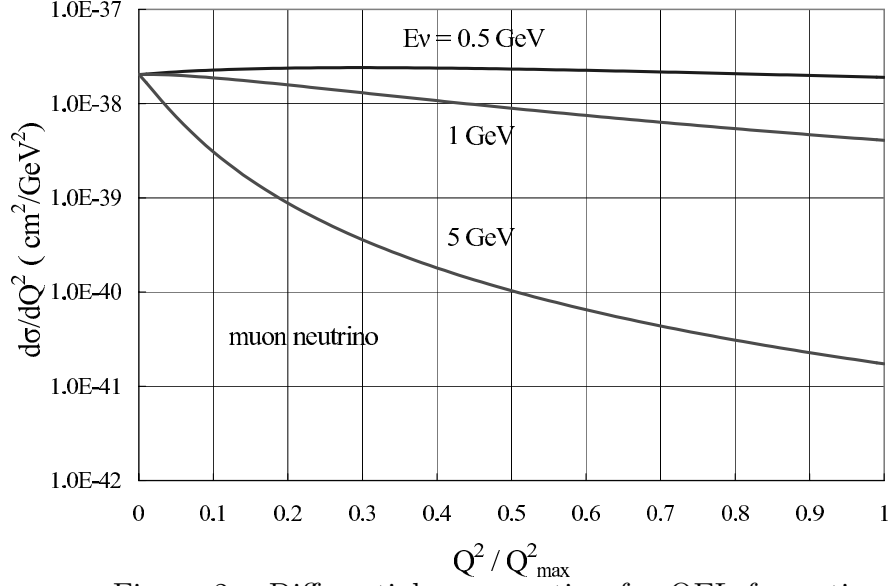


Figure 2: Differential cross section for QEL for anti-muon neutrinos with the same incident energies as in Fig. 1.

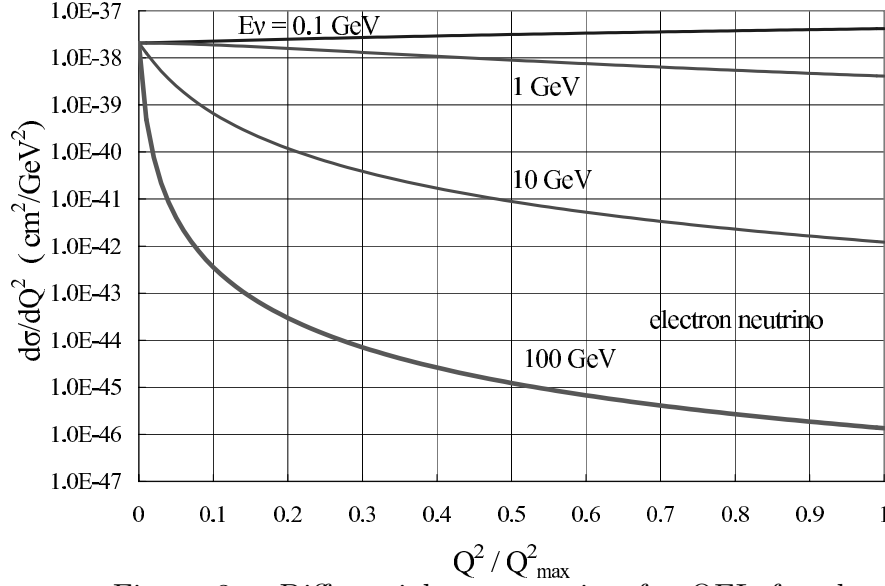


Figure 3: Differential cross section for QEL for electron neutrinos with different incident energies, 0.1 GeV, 1 GeV, 10 GeV and 100 GeV.

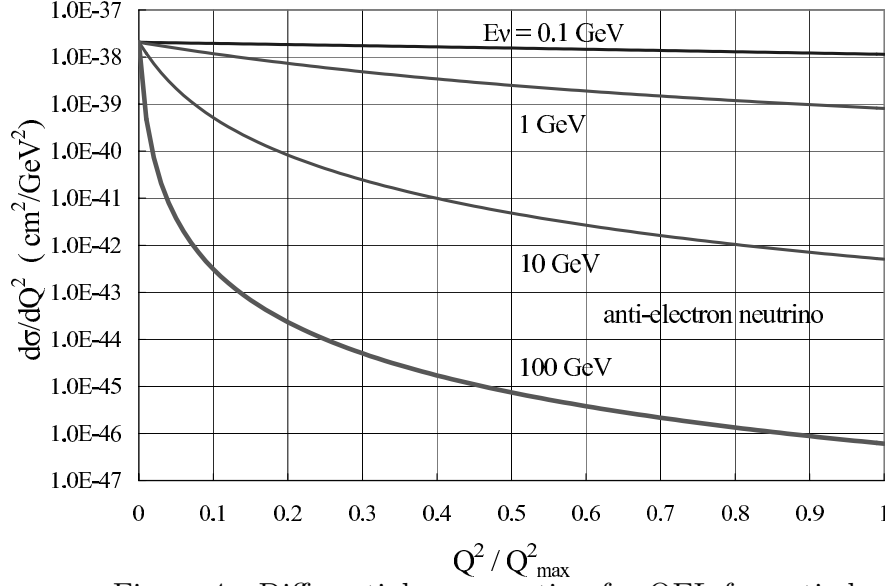


Figure 4: Differential cross section for QEL for anti-electron neutrinos with the same incident energies as in Fig. 3.

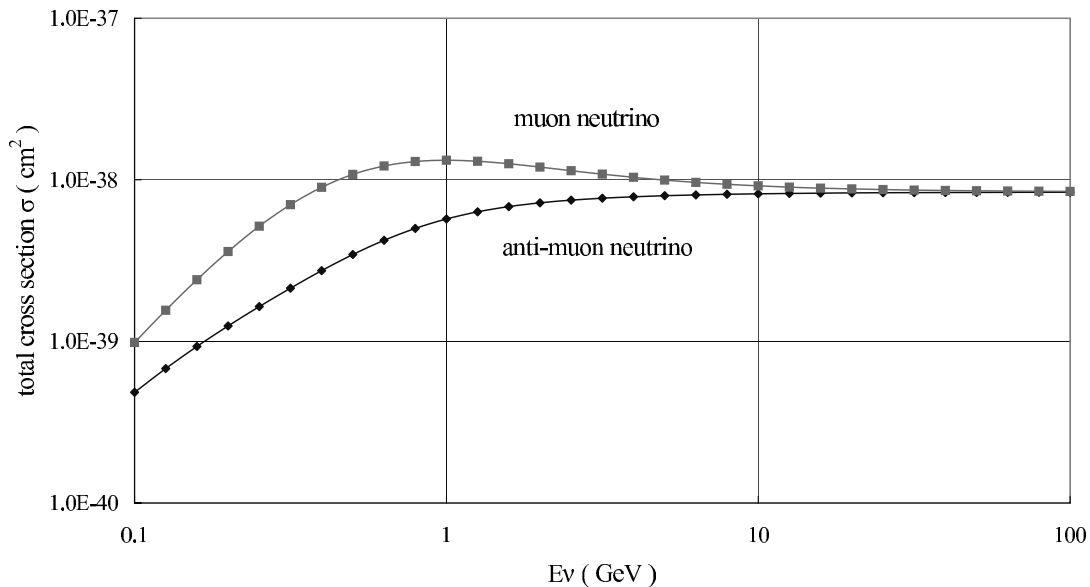


Figure 5: Total cross sections of QEL for muon neutrino and anti-muon neutrino as a function of the incident neutrino energy.

It can be seen from Eqs. (3) and (4) that there is a relation between the energy E_ℓ of the charged lepton and its scattering angle θ_s for a given incident neutrino energy E_ν . Figure 6 shows this relation for muon, from which we can easily understand that the scattering angle θ_s of the charged lepton (muon here) cannot be neglected. For a quantitative examination of the scattering angle, we construct the distribution function for θ_s of the charged lepton from Eqs. (2) to (4) by using the Monte Carlo method.³

Figure 7 gives the distribution function for θ_s of the muon produced in the muon neutrino interaction. It can be seen that the muons produced from lower energy neutrinos are scattered over wider angles and that a considerable part of them are scattered even in backward directions. Similar results are obtained for anti-muon neutrinos, electron neutrinos and anti-electron neutrinos.

Also, in a similar manner, we obtain not only the distribution function for the scattering angle of the charged leptons, but also their average values $\langle \theta_s \rangle$ and their standard deviations σ_s . Table 1 shows them for muon neutrinos, anti-muon

³The distribution functions for the scattering angle can be more easily obtained by the numerical method than done by the Monte Carlo method. The reason why we obtain them by the Monte Carlo method is to apply this Monte Carlo simulation procedure to another purpose by which we get the essential part of this paper. The distribution function for scattering angle in the inelastic scattering of the neutrino interaction and other quantities had been obtained by Kobayakawa *et al.* See [7].

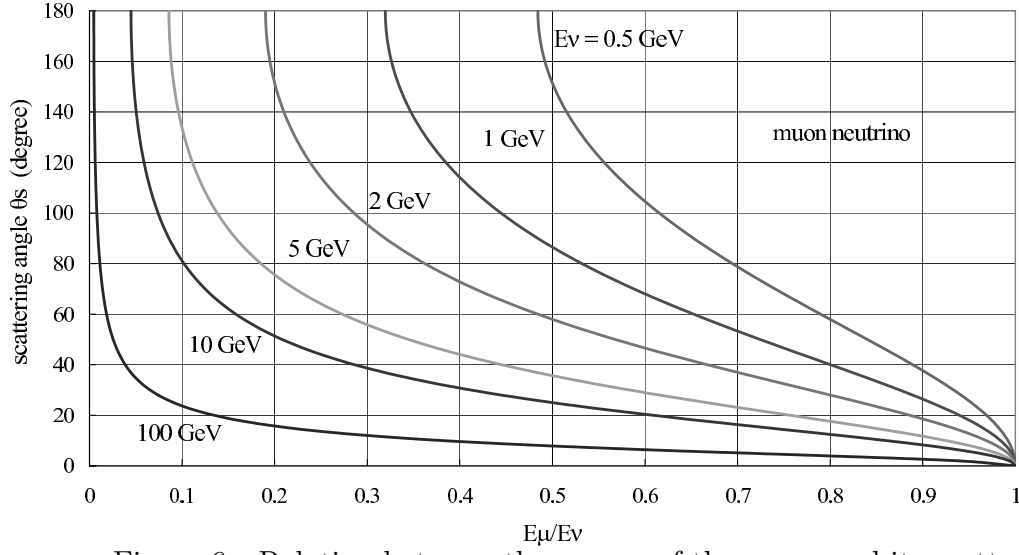


Figure 6: Relation between the energy of the muon and its scattering angle for different incident muon neutrino energies, 0.5 GeV, 1 GeV, 2 GeV, 5 GeV, 10 GeV and 100 GeV.

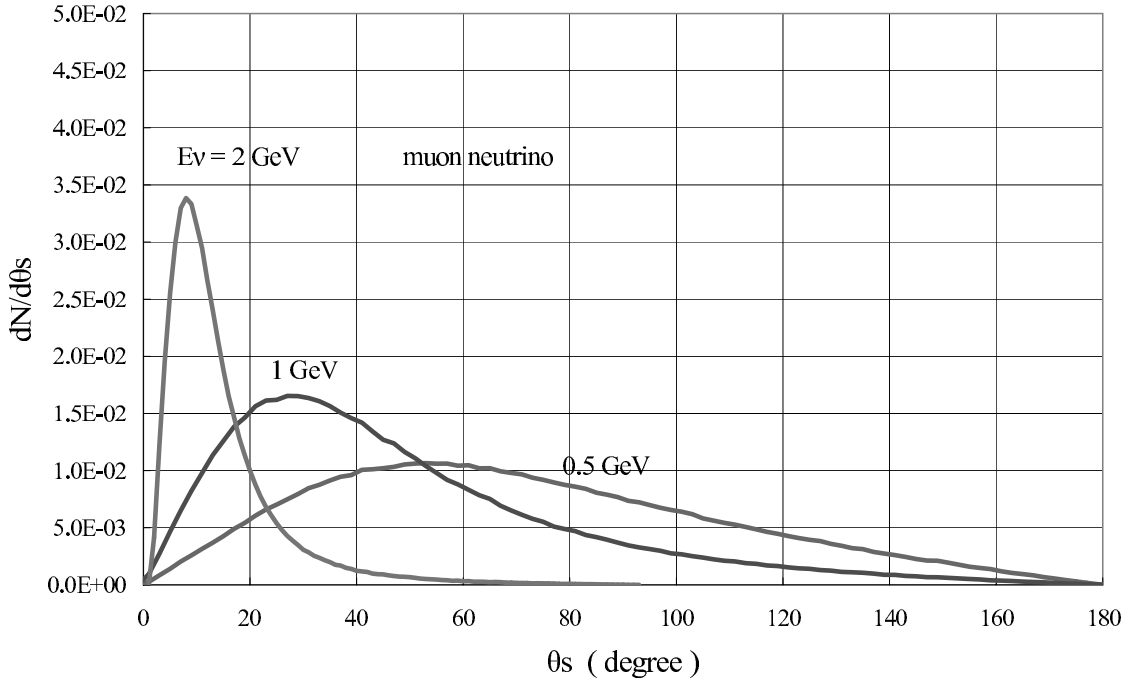


Figure 7: Distribution functions for the scattering angle of the muon for muon-neutrino with incident energies, 0.5 GeV, 1.0 GeV and 2 GeV. Each curve is obtained by the Monte Carlo method (one million sampling per each curve).

Table 1: The average values $\langle \theta_s \rangle$ for scattering angle of the emitted charged leptons and their standard deviations σ_s for various primary neutrino energies E_ν .

E_ν (Gev)	angle (degree)	ν_μ	$\bar{\nu}_\mu$	ν_e	$\bar{\nu}_e$
0.2	$\langle \theta_s \rangle$	89.86	67.29	89.74	67.47
	σ_s	38.63	36.39	38.65	36.45
0.5	$\langle \theta_s \rangle$	72.17	50.71	72.12	50.78
	σ_s	37.08	32.79	37.08	32.82
1	$\langle \theta_s \rangle$	48.44	36.00	48.42	36.01
	σ_s	32.07	27.05	32.06	27.05
2	$\langle \theta_s \rangle$	25.84	20.20	25.84	20.20
	σ_s	21.40	17.04	21.40	17.04
5	$\langle \theta_s \rangle$	8.84	7.87	8.84	7.87
	σ_s	8.01	7.33	8.01	7.33
10	$\langle \theta_s \rangle$	4.14	3.82	4.14	3.82
	σ_s	3.71	3.22	3.71	3.22
100	$\langle \theta_s \rangle$	0.38	0.39	0.38	0.39
	σ_s	0.23	0.24	0.23	0.24

neutrinos, electron neutrinos and anti-electron neutrinos. In the SK analysis, it is assumed that the scattering angle of the charged particle is zero [3, 4], but Table 1 demonstrates that such an assumption does not hold at all in both *Fully Contained Events* and *Partially Contained Events*.

Therefore, it is surely concluded that the zenith angle distribution obtained by SK for *Fully Contained Events* and *Partially Contained Events* are almost unreliable, which will be shown later more concretely.

3 Influence of Azimuthal Angle of Quasi Elastic Scattering over the Zenith Angle of the Fully Contained Events

For three incident cases (vertical, horizontal and diagonal), Fig. 8 gives a schematic representation of the relationship among the zenith angle of the incident neutrino, θ_ν , the scattering angle of the charged lepton, θ_s , and the azimuthal angle of the charged lepton, ϕ . In this paper, we measure θ_ν from the vertical upward direction.

From Fig. 8-a, it can be seen that the zenith angle θ of the charged lepton is not influenced by its ϕ in the vertical incidence ($\theta_\nu = 0^\circ$). From Fig. 8-b, however, it is obvious that the angle ϕ influences on its zenith angle greatly in the case of horizontal incidence of the neutrino ($\theta_\nu = 90^\circ$). Namely, half of the charged leptons are recognized as upward going, while the other half is classified as downward going. The intermediate case (diagonal incidence of $\theta_\nu = 43^\circ$) between the above two cases is shown in Fig. 8-c. As discussed above, we must take account of the effect due to the azimuthal angle ϕ in the analysis of both *Fully Contained Events* and *Partially Contained Events*. Figure 9 shows the relation between direction cosines of the incident neutrinos, (ℓ, m, n) , and those of the charged lepton, (ℓ_r, m_r, n_r) , for certain θ_s and ϕ . Then, we have the following expression:

$$\begin{pmatrix} \ell_r \\ m_r \\ n_r \end{pmatrix} = \begin{pmatrix} \frac{\ell n}{\sqrt{\ell^2 + m^2}} & -\frac{m}{\sqrt{\ell^2 + m^2}} & \ell \\ mn & \frac{\ell}{\sqrt{\ell^2 + m^2}} & m \\ \frac{\sqrt{\ell^2 + m^2}}{-\sqrt{\ell^2 + m^2}} & 0 & n \end{pmatrix} \begin{pmatrix} \sin\theta_s \cos\phi \\ \sin\theta_s \sin\phi \\ \cos\theta_s \end{pmatrix}, \quad (5)$$

where $n = \cos\theta_\nu$, and $n_r = \cos\theta$. Here, θ is the zenith angle of the charged lepton.

Using Eq. (5), we carry out a Monte Carlo calculation to examine the influence of ϕ on θ for the charged lepton. The Monte Carlo procedure for the determination of the real θ of the charged lepton whose parent (anti-)neutrino has fixed θ_ν and E_ν involves the following steps:

1. We extract Q^2 from the probability function for the differential cross section with a given E_ν (Eq. (2)) by the random sampling.
2. We obtain E_ℓ from Eq. (4).
3. We obtain θ_s from Eq. (3).
4. We decide ϕ , which is obtained from

$$\phi = 2\pi\xi. \quad (6)$$

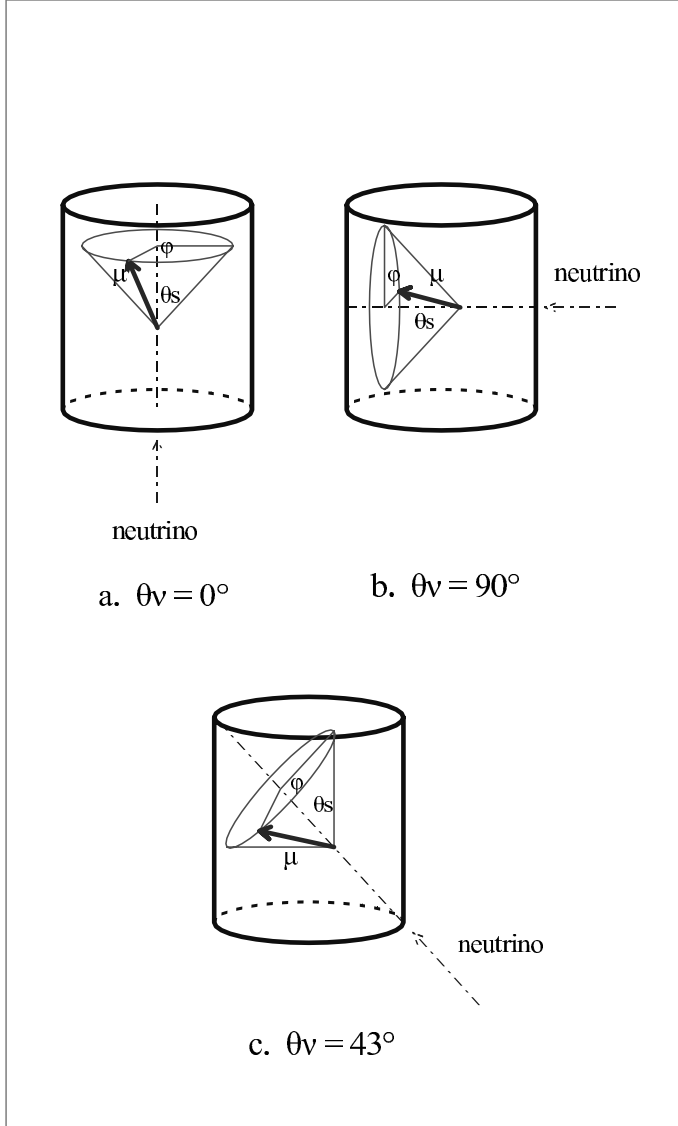


Figure 8: Schematic view of the zenith angles of the charged muons for different zenith angles of the incident neutrinos, focusing on their azimuthal angles.

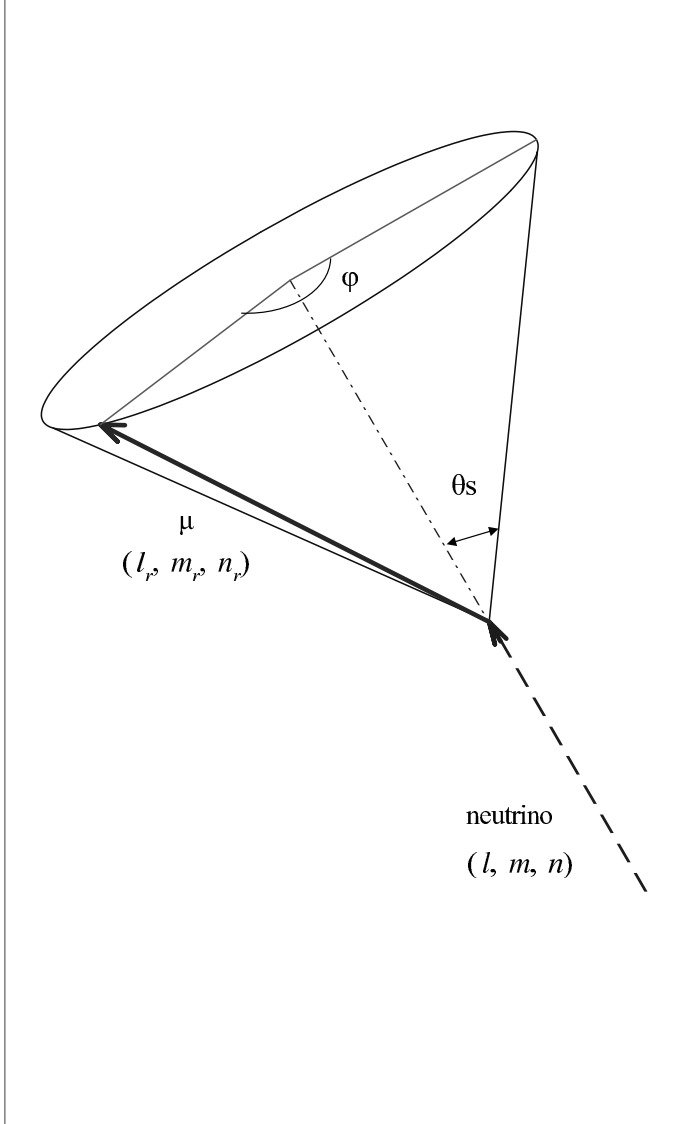


Figure 9: The relation between the direction cosines of the incident neutrino and those of the emitted charged lepton.

Here, ξ is a uniform random number between 0 and 1.

5. We obtain (ℓ_r, m_r, n_r) by using Eq. (5). The n_r is the cosine of the zenith angle of the charged lepton which should be contrasted to n , that of the incident neutrino. In the SK analysis, it is assumed that

$$(\ell_r, m_r, n_r) = (\ell, m, n). \quad (7)$$

We examine θ , the zenith angles of the charged muons, for three typical zenith angles of the incident neutrino with $E_\nu = 1$ GeV, namely, $\cos \theta_\nu = 1$ (vertically upward), $\cos \theta_\nu = 0.731$, i.e., $\theta_\nu = 43^\circ$ (diagonal in SK), and $\cos \theta_\nu = 0$ (horizontal).

A : vertically upward incident neutrino events

In this case, as easily understood from Fig. 8-a, we can skip the step 4 mentioned above, because the change of ϕ of the charged muon has no influence over its zenith angle θ .

Here, although the direction of the charged muon approximately retains the primary direction of the incident neutrino at higher energies, say, above ~ 20 GeV, it deviates from the primary direction (vertical), even to backward directions, at lower energies, say, below ~ 1 GeV (see also Fig. 7).

In Fig. 10, we show the scatter plot between E_μ , the emitted energy of the charged muon and $\cos \theta$, the cosine of the zenith angle of the charged muon for the vertically incident neutrino. In this case, the relation between θ and E_ν is unique because of independence of the azimuthal angle. The reason is as follows: For a given Q^2 (see Eq.(2)) we obtain the energy of the charged lepton and its scattering angle uniquely due to the two body kinematics and the zenith angle of the charged lepton are never influenced from their azimuthal angle, because θ is measured from the vertical direction, parallel to the axis of the detector.

B: horizontally incident neutrino events

This case shows a great contrast to the vertical case. In Fig. 11, we give the scatter plot between E_ν and $\cos \theta$. In this case, the influence of ϕ over θ is the strongest among the three, because this influence appears through Eq.(5) as strongly as possible. The $\cos \theta$ has the widest distribution, even if the charged muon has the same energy. As θ is symmetrical due to its azimuthal symmetry, the scattered muons have almost lost the direction of primary neutrinos at lower energies, say, ~ 1 GeV and show a uniform distribution between upward and downward. It should be noted that the scatter plots are distributed symmetrically around $\cos \theta = 0$, reflecting the azimuthal symmetry.

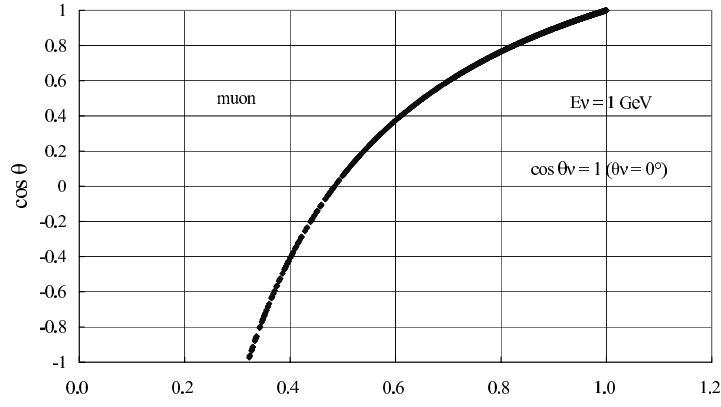


Figure 10: The scatter plot between the fractional energies of the produced muons and their zenith angles for vertically incident muon neutrinos with 1 GeV. The sampling number is 1000.

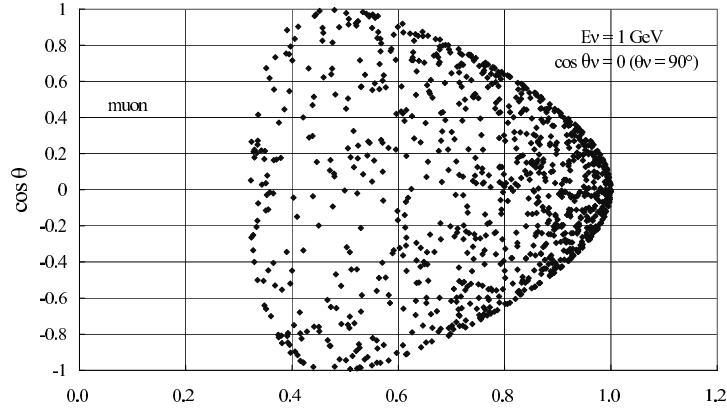


Figure 11: The scatter plot between the fractional energies of the produced muons and their zenith angles for horizontally incident muon neutrinos with 1 GeV. The sampling number is 1000.

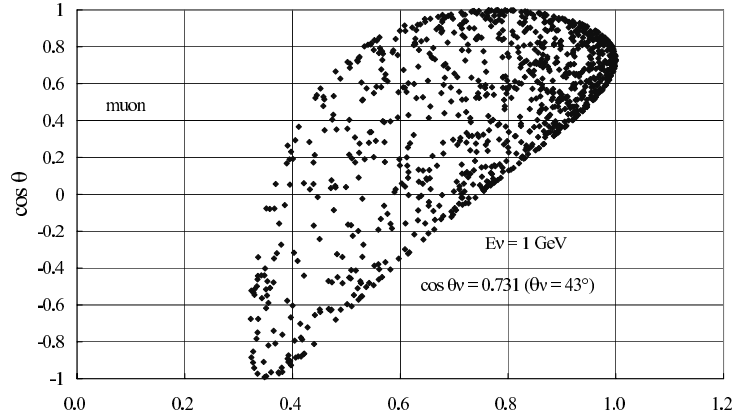


Figure 12: The scatter plot between the fractional energies of the produced muons and their zenith angles for diagonally incident muon neutrinos with 1 GeV. The sampling number is 1000.

C: diagonally upward incident neutrino events

In Fig. 12, we show the similar scatter plot for the diagonal case, which shows the intermediate situation between Figs. 10 and 11, as expected. From Fig. 12 for $\theta_\nu = 43^\circ$, it is still apparent that ϕ influences θ in a considerable degree, even if the energies of the charged muon are the same.

We can get the similar scatter plots for electrons to those for muons.

We sum the events concerned over E_ℓ for a given $\cos\theta$ in Figs 10 to 12 and show the results of the zenith angle distribution in Figs 13 to 15. In Fig. 13, the neutrino enters vertically. In this case, even if we define $\cos\theta = 0.8 \sim 1.0$ as “vertical”, about one half of the real events are not recognized as vertical. In Fig. 14 we give the zenith angle distribution for the horizontal($\cos\theta_\nu = 0$). Comparing it with Fig. 13, it is easily understood that the direction of the primary neutrino here has been almost completely lost, namely, n_r is very different from n . Thus, the SK assumption ($n_r = n$) clearly does not hold in this energy region. In Fig. 15, we show the intermediate state between Figs. 13 and 14. The tendencies in Figs. 13 to 15 for muon neutrinos are quite similar to those for electron neutrinos.

Furthermore, the dependence of $\cos\theta$ on $\cos\theta_\nu$ becomes more sensitive at lower energies, say, below ~ 0.2 GeV. Also, they are a little weaker for anti-neutrinos than for neutrinos, as can be inferred from the cross sections in Figs. 1 to 4 and Fig. 5.

It should be, here, emphasized that the azimuthal angle of the charged lepton greatly influences discrimination between *Fully Contained Events* and *Partially Contained Events*, which is strongly dependent on the generation points of the neutrino events concerned. The estimation of this discrimination is very important for getting *Fully Contained Events*, because the correct analysis of *Fully Contained Events* only in the SK experiment makes it possible to lead less ambiguous conclusion on neutrino oscillation. @

4 The Zenith Angle of Fully Contained Events Taking Account of the Overall Neutrino Spectrum

In the previous section, we obtain the zenith angle distribution of both *Fully Contained Events* and *Partially Contained Events* for a given energy of the incident neutrino, taking account of the effect of the azimuthal angle for a given zenith angle of the incident neutrino. However, in order to examine the effect of θ_s and

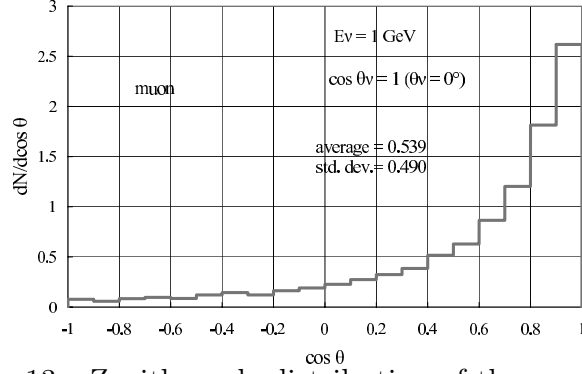


Figure 13: Zenith angle distribution of the muon for the vertically incident muon neutrino with 1 GeV. The sampling number is 10000.

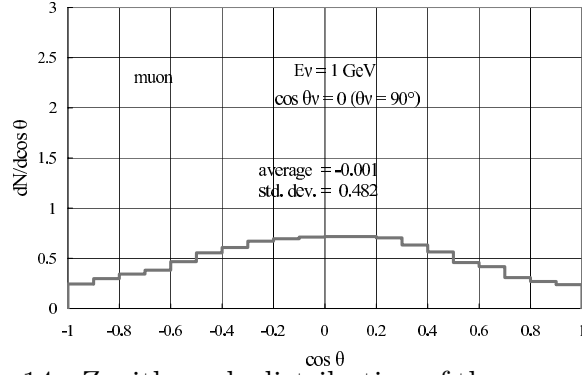


Figure 14: Zenith angle distribution of the muon for the horizontally incident muon neutrino with 1 GeV. The sampling number is 10000.

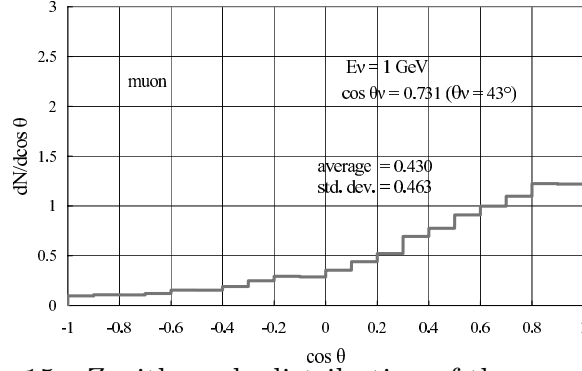


Figure 15: Zenith angle distribution of the muon for the diagonally incident muon neutrino with 1 GeV. The sampling number is 10000.

ϕ of the charged lepton in QEL on the direction of primary neutrinos, we must consider the overall neutrino spectrum, not a fixed neutrino energy.

The concrete procedures for a selected event with a given θ_ν of the incident neutrino are summarized again as follows:

Procedure A

We formulate the differential neutrino interaction probability functions for muon (electron) and anti-muon (anti-electron) in which the (anti-)neutrino differential energy spectra are combined with the total cross sections of the corresponding neutrino concerned for QEL. In such a calculation, the differential neutrino spectra at Kamioka site which cover from 0.1 GeV to 100 GeV obtained by Fiorentini *et al.*[8] are utilized.

Procedure B

The determination as to whether the (anti-)neutrino concerned belongs to either neutrino or to anti-neutrino is done by random sampling according to the probability functions constructed from Procedure A.

Procedure C

We randomly sample the energy of the (anti-)neutrino concerned according to the probability function constructed from the Procedure A.

Procedure D

We randomly sample Q^2 from Eq. (2) whose neutrino energy is determined by Procedure C.

Procedure E

We decide the energy of the charged lepton concerned, E_ℓ , for the Q^2 from Eq. (4).

Procedure F

We decide the scattering angle of the charged lepton concerned, θ_s , from Eq. (3).

Procedure G

We randomly sample the azimuthal angle of the charged lepton concerned, ϕ , from Eq. (6).

Procedure H

We decide the direction cosines of the charged lepton concerned by using Eq. (5), being accompanied by Procedures F and G.

We repeat Procedures B to H until we reach the desired trial number.

In Figs. 16 to 18, we give the zenith angle distributions of the sum of μ^+ and μ^- for a given zenith angle of parent neutrinos. In Figs. 19 to 21, we give those for e^+ and e^- which correspond to Figs. 16 to 18. There are no major differences between (anti-)muon and (anti-)electron. The small differences between them are mainly due to the different neutrino fluxes between (anti-)muon neutrinos and (anti-)electron neutrinos.

If the SK assumption is valid, then, the zenith angle distribution of the charged leptons should be of the delta function type. However, the real distributions of the charged leptons in Figs. 16 to 21 are quite far from the delta function type distribution. From Figs. 16 to 21, we can conclude that the present SK analysis procedures for *Fully Contained Events* and *Partially Contained Events* can not essentially determine the zenith angles of the incident neutrinos. It should be finally noticed that we must consider not only the contribution of the downward neutrino events which originate from the upward going neutrinos, but also that of the upward neutrino events which originate from the downward going neutrinos.

5 Conclusions

The standard SK analysis for *Fully Contained Events* and *Partially Contained Events* assumes that the direction of the emitted charged lepton is the same as that of the incident neutrino. However, Figs. 16 to 22 clearly show that the zenith angle distributions of the charged leptons have a wide spread for a fixed zenith angle of the incident (anti-)neutrino, with the leptons even being scattered backward in some cases, while the corresponding distributions obtained from the SK assumption should be of the delta function type, the peak of which correspond to the zenith angles of the incident neutrinos.

Thus, it is clearly shown that the real zenith angle distribution of the charged particle in which their scattering angle is correctly taken into account cannot be approximated in any sense to the delta function type distribution which comes directly from the SK assumption.

Consequently, the SK assumption ($n_r = n$) does not reflect the real zenith angle for directions of the incident neutrinos.

Namely, our results show clearly that the zenith angle distribution of the muon-like (single ring) events and electron-like (single ring) events cannot reflect that of incident neutrinos, even if the discrimination between electron and muon is perfect.

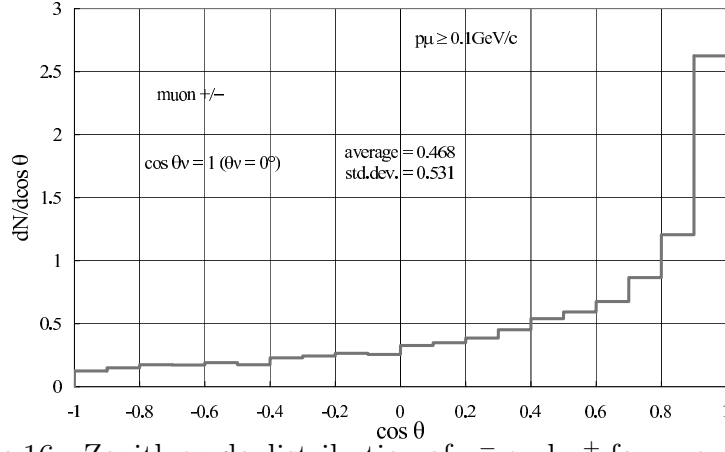


Figure 16: Zenith angle distribution of μ^- and μ^+ for ν_μ and $\bar{\nu}_\mu$ with the vertical direction, taking account of the overall neutrino spectrum at Kamioka site. The sampling number is 10000.

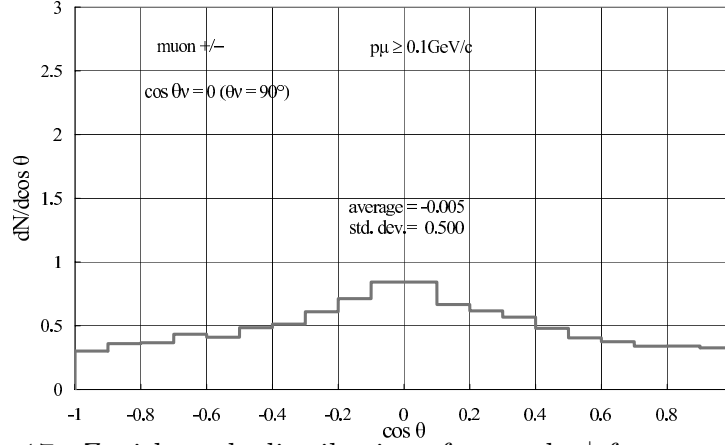


Figure 17: Zenith angle distribution of μ^- and μ^+ for ν_μ and $\bar{\nu}_\mu$ with the horizontal direction, taking account of the overall neutrino spectrum at Kamioka site. The sampling number is 10000.

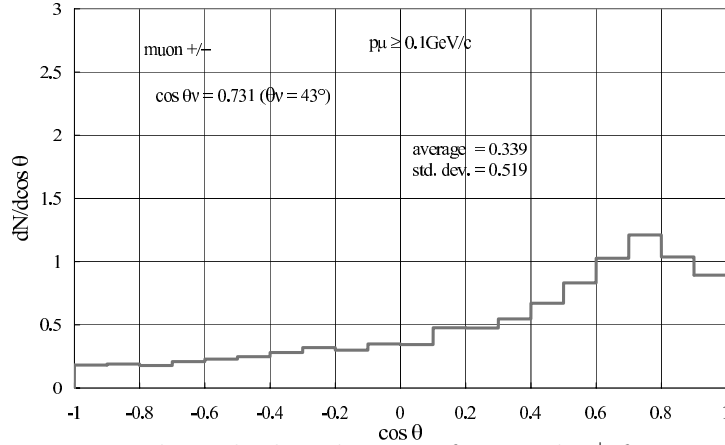


Figure 18: Zenith angle distribution of μ^- and μ^+ for ν_μ and $\bar{\nu}_\mu$ with the diagonal direction, taking account of the overall neutrino spectrum at Kamioka site. The sampling number is 10000.

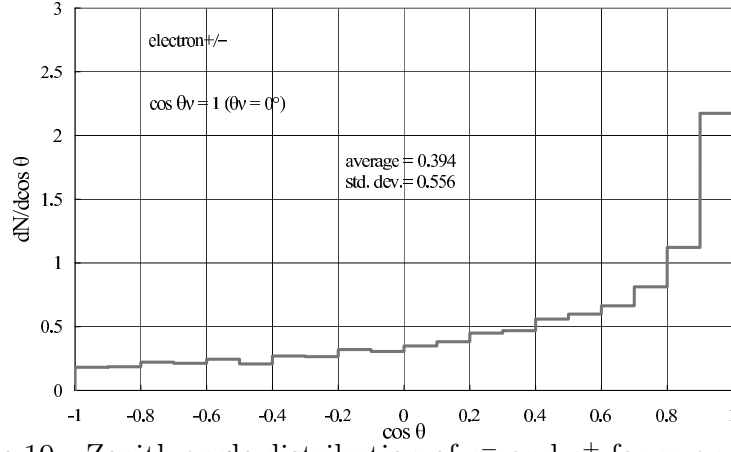


Figure 19: Zenith angle distribution of e^- and e^+ for ν_e and $\bar{\nu}_e$ with the vertical direction, taking account of the overall neutrino spectrum at Kamioka site. The sampling number is 10000.

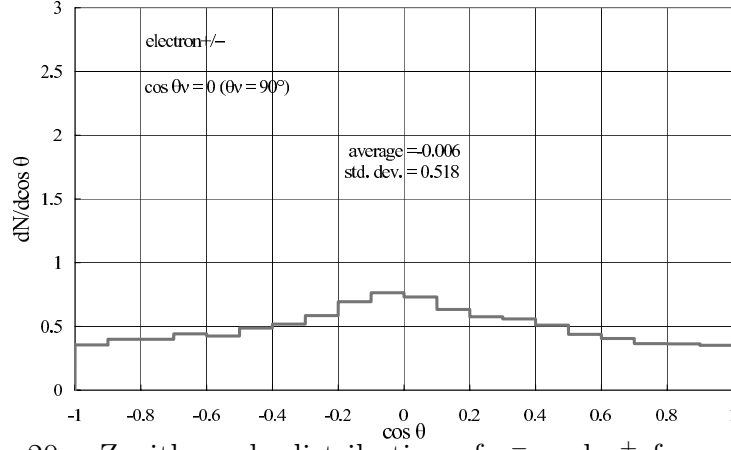


Figure 20: Zenith angle distribution of e^- and e^+ for ν_e and $\bar{\nu}_e$ with the horizontal, taking account of the overall neutrino spectrum at Kamioka site. The sampling number is 10000.

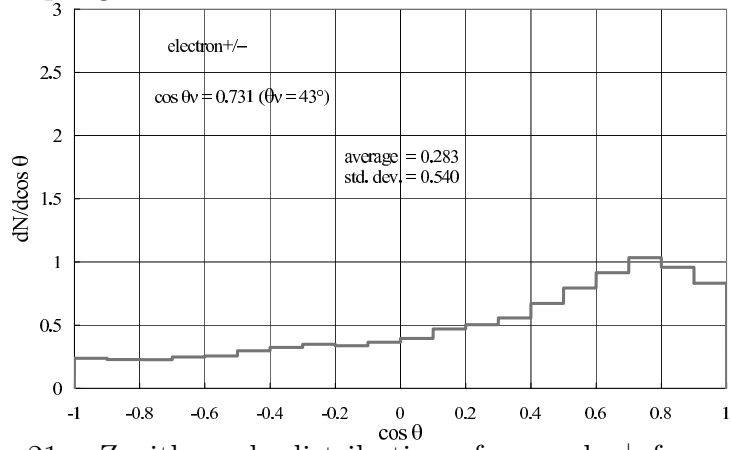


Figure 21: Zenith angle distribution of e^- and e^+ for ν_e and $\bar{\nu}_e$ with the diagonal, taking account of the overall neutrino spectrum at Kamioka site. The sampling number is 10000.

The zenith angle distribution of both *Fully Contained Events* and *Partially Contained Events* in our numerical computer experiment in which the polar angle (the scattering angle) as well as the azimuthal angle of the charged leptons are correctly taken into account will be published elsewhere.

⁴We have studied the SK discrimination between electrons and muons by simulating electron-like (single ring) events and muon-like (single ring) events and examining the discrimination between them, based on the concept of pattern recognition. We conclude that the level of discrimination claimed by SK is practically impossible to achieve. This study will be described in a later publication.

References

- [1] Kasuga, S. *et al.*, Phys. Lett. **B374** (1996) 238.
- [2] Fukuda, Y. *et al.*, Phys. Rev. Lett. **81** (1998) 1562.
Fukuda, Y. *et al.*, Phys. Rev. Lett. **82** (1999) 2642.
- [3] Kajita, T. and Totsuka, Y. Rev. Mod. Phys., **73** (2001) 85. See p. 101.
- [4] Ishitsuka, M., PhD thesis, University of Tokyo (2004). See p. 138.
- [5] Lipari, P., Lusignoli, M. and Sartogo, F., Phys. Rev. Lett. **74** (1995) 4384.
- [6] Renton, P., *Electro-weak Interaction*, Cambridge University Press (1990). See p. 405.
- [7] Kobayakawa, K., Numata, N. and Sumura, T., 21th ICRC Proc.9 (1990) 413.
- [8] Fiorentini, G., Naumov, V.A. and Vilante, F.L., Phys. Lett. **B510** (2001) 173.